



The IL-6–gp130–STAT3 pathway in hepatocytes triggers liver protection in T cell–mediated liver injury

Christian Klein,¹ Torsten Wüstefeld,¹ Ulrike Assmus,¹ Tania Roskams,² Stefan Rose-John,³ Michael Müller,⁴ Michael P. Manns,¹ Mattias Ernst,⁵ and Christian Trautwein¹

¹Department of Gastroenterology, Hepatology and Endocrinology, Hannover Medical School, Hanover, Germany. ²Head Liver Research Unit, Department of Pathology, University of Leuven, Leuven, Belgium. ³Department of Biochemistry, Christian-Albrechts-Universität Kiel, Medical Faculty Kiel, Germany. ⁴Nutrition, Metabolism & Genomics Group, Division of Human Nutrition, Wageningen University, Wageningen, The Netherlands. ⁵Ludwig Institute for Cancer Research, PO Royal Melbourne Hospital, Melbourne, Victoria, Australia.

Increasing evidence demonstrates that IL-6 has a protective role during liver injury. IL-6 activates intracellular pathways via the gp130 receptor. In order to identify IL-6–gp130 pathways involved in mediating liver protection, we analyzed hepatocyte-specific gp130 knockout mice in a concanavalin A–induced (Con A–induced) model of immune-mediated hepatitis. We demonstrated that IL-6–gp130–dependent pathways in hepatocytes alone are sufficient for triggering protection in Con A–induced hepatitis. gp130–STAT3 signaling in hepatocytes mediates the IL-6–triggered protective effect. This was demonstrated by analysis of IL-6–induced protection in mice selectively deficient for gp130–dependent STAT1/3 or gp130–SHP2–RAS signaling in hepatocytes. To identify IL-6–gp130–STAT1/3 dependently expressed liver-protective factors, we performed gene array analysis of hepatic gene expression in hepatocyte-specific gp130^{-/-} mice as well as in gp130–STAT1/3– and gp130–SHP2–RAS–MAPK–deficient mice. The mouse IL-8 ortholog KC (also known as Gro- α) and serum amyloid A2 (SAA2) was identified as differentially IL-6–gp130–STAT3–regulated genes. Hepatic expression of KC and SAA2 mediate the liver-protective potential of IL-6, since treatment with recombinant KC or serum SAA2 effectively reduced liver injury during Con A–induced hepatitis. In summary, this study defines IL-6–gp130–STAT3–dependent gene expression in hepatocytes that mediates IL-6–triggered protection in immune-mediated Con A–induced hepatitis. Additionally, we identified the IL-6–gp130–STAT3–dependent proteins KC and SAA2 as new candidates for therapeutic targets in liver diseases.

Introduction

Various etiologies result in acute and chronic liver diseases. Particularly in autoimmune and viral hepatitis, immune-mediated mechanisms play a central role and thus determine disease progression. In recent years, major progress has been made in treating these patients. However, there are still a high percentage of individuals for whom all treatment options fail and liver transplantation is required. Therefore, alternative treatment options are needed; therapeutic approaches that either inhibit immune-mediated mechanisms or directly inhibit liver cell damage are promising and might enter into the clinic.

IL-6 is a pleiotropic cytokine with beneficial effects for the liver. This cytokine promotes liver regeneration and protects against a multitude of liver-damaging influences such as alcohol and CCl₄ intoxication (1–4). IL-6 prevents apoptosis and exhibits positive effects in both ischemia/reperfusion models and fatty liver transplantation (5–7). Additionally, IL-6 is known to efficiently reduce the increase of serum transaminases (ASTs) in the concanavalin A (Con A) mouse model of T cell–mediated hepatitis (1).

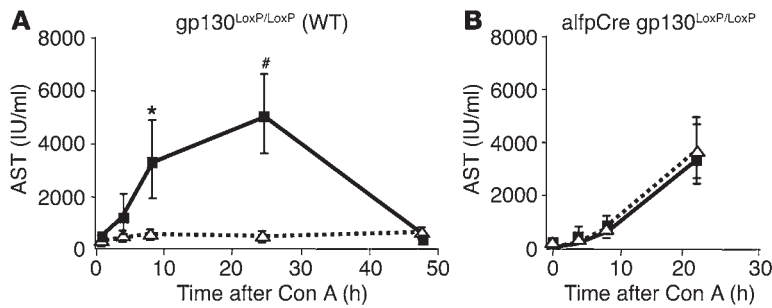
Con A–induced liver damage is a well-defined experimental animal model of acute hepatitis. It mimics human viral and autoimmune hepatitis in many aspects (8–10). Con A–induced hepatitis is accompanied by an increase in the serum concentration of several cytokines, including TNF- α , IFN- γ , IL-6, and IL-1. During the early stages, TNF- α and IFN- γ directly mediate liver cell damage (11). The cell types involved in the initiation and propagation of Con A–induced hepatitis (neutrophils: CD4⁺ T cells, CD8⁺ T cells, NK T cells [NKT cells], and Kupfer cells) have been directly implicated in a number of human liver diseases, including autoimmune, viral, alcoholic, and ischemia/reperfusion injury (12–18).

The IL-6–triggered molecular mechanisms leading to liver protection are not completely understood. For signal transduction, IL-6 binds the membrane-bound IL-6 receptor α (gp80). The IL-6–gp80 dimer interacts with gp130, the signal transducing unit in this complex. Gp130 is the common signal transducer used by the IL-6 family of cytokines, which includes IL-6, leukemia inhibitory factor (LIF), IL-11, cardiotrophin-1 (CT-1), oncostatin-M (OSM), and the ciliary neurotrophic factor (19). The initiated intracellular signaling is strictly dependent on the function of gp130 (19). Formation of gp130-containing complexes results in activation of intracellular JAKs, which phosphorylate tyrosine residues in the cytoplasmic domain of gp130. The phosphorylation of gp130 leads to dimerization of gp130 and activation of STAT1 and STAT3 as well as the SHP2–RAS–MAPK pathway (where SHP2 is Src homology 2 [SH2] domain–containing protein tyrosine phosphatase) (20–22). The use of distinct downstream signaling pathways from different

Nonstandard abbreviations used: AST, serum transaminase; Con A, concanavalin A; CT-1, cardiotrophin-1; KC, keratinocyte growth factor; NKT cell, NK T cell; OSM, oncostatin-M; PMN, polymorph nuclear cell; SAA2, serum amyloid A2; SH2, Src homology 2; SHP2, Src homology 2 domain–containing protein tyrosine phosphatase.

Conflict of interest: The authors have declared that no conflict of interest exists.

Citation for this article: *J. Clin. Invest.* 115:860–869 (2005). doi:10.1172/JCI200523640.

**Figure 1**

gp130 in hepatocytes is essential for IL-6-dependent protection in Con A-induced hepatitis. Con A hepatitis was induced by intravenous injection of 32.5 mg/kg Con A in wild-type (gp130^{LoxP/LoxP}) and hepatocyte-specific gp130-null (alfpCre gp130^{LoxP/LoxP}) mice. Mice were pretreated for 3 hours with NaCl (solid line) or IL-6 (200 µg/kg) (dotted line) before i.v. injection of Con A. Liver injury was quantified by detection of AST. (A) Time course of AST serum levels during Con A-induced hepatitis in wild-type mice pretreated with NaCl (solid line) or IL-6 (dotted line). #*P* < 0.01 and **P* < 0.05 vs. corresponding IL-6-pretreated wild-type control group at the same time point. (B) Time course of AST serum levels during Con A-induced hepatitis in alfpCre gp130^{LoxP/LoxP} mice pretreated with NaCl (solid line) or IL-6 (dotted line).

phosphorylation sites of the gp130 intracellular domain enables ligand- and tissue-specific activation of specific target genes. For these reasons, IL-6 signaling allows a complex plasticity (23, 24).

The aim of the present study is to identify the IL-6–gp130-dependent pathways and the cell type that confer protection during Con A-induced liver injury. The identification of the responsible target cell and the essential intracellular signal cascade will help to clarify liver protective mechanisms and to identify IL-6-dependent molecular mediators that contribute to beneficial effects in immune-mediated liver diseases.

Results

IL-6–gp130-dependent signaling in hepatocytes confers protection in the Con A model. The cytokine IL-6 triggers liver protection in the Con A model of T cell-mediated hepatitis. IL-6 controls gene transcription in various cell types that might be involved in protective mechanisms, e.g., hepatocytes and immune-activated cells. Hepatocytes are the predominant hepatic cells; therefore, we evaluated whether hepatocytes mediate IL-6-dependent protection in the Con A model. We generated mice with a hepatocyte-specific deletion of the IL-6 signal-transducing gp130 receptor (25) and analyzed the effect of IL-6 treatment in this experimental hepatitis model. Hepatocyte-specific gp130-deficient mice were generated by crossbreeding alfpCre and gp130loxP mice, in which LoxP sites flank exon 16, encoding the transmembrane domain of gp130 (26). Expression of Cre recombinase is controlled by a hepatocyte-specific albumin promoter, and results in a more than 90% deletion of exon 16 in adult liver (25). Since nonparenchymal cells show no gp130 deletion, the overall extent of hepatic gp130 inactivation is likely to reflect complete gp130 deletion in hepatocytes.

Gp130 wild-type (gp130^{LoxP/LoxP}) animals were treated with IL-6 or vehicle before Con A injection. In order to monitor liver cell damage, AST levels were determined before and at various time points after treatment. IL-6 pretreatment completely blocked liver cell damage. No increase in transaminases was evident (Figure 1A). In alfpCre gp130^{LoxP/LoxP} mice, IL-6 failed to have a protective effect, which indicates that IL-6-dependent liver protection is dependent on

gp130-mediated signaling in hepatocytes (Figure 1B). Additionally, all alfpCre gp130^{LoxP/LoxP} mice died within the first 20 hours after Con A injection. In contrast, all NaCl- and IL-6-treated wild-type animals survived during this phase, indicating a higher sensitivity of alfpCre gp130^{LoxP/LoxP} mice toward Con A.

Lack of gp130 expression in hepatocytes has no impact on liver-damaging cytokine secretion after Con A injection. During Con A-induced hepatitis, immune cells are activated, and as a consequence, cytokines that promote liver cell damage are released. TNF-α and IFN-γ are essential in triggering Con A-induced liver injury. Additionally, IFN-γ and TNF-α are markers of immune-cell activation in this model. They are expressed by activated macrophages or CD4⁺ and CD8⁺ cells (1, 3, 27, 28). Therefore, we were interested in studying whether lack of gp130 expression in hepatocytes and IL-6 pretreatment have an impact on cytokine secretion.

IL-6 treatment of gp130^{LoxP/LoxP} mice resulted in a slight reduction of TNF-α levels compared with those in animals treated with the carrier solution (Figure 2A). The same observation was evident in alfpCre gp130^{LoxP/LoxP} animals. Slightly reduced TNF-α levels were observed in the IL-6-treated group (Figure 2B). IL-6 pretreatment had no impact on IFN-γ secretion in wild-type and alfpCre gp130^{LoxP/LoxP} animals (Figure 2, C and D).

The endogenous IL-6 levels during Con A-induced hepatitis are significantly elevated in alfpCre gp130^{LoxP/LoxP} mice. In wild-type mice, a significant increase in IL-6 serum concentration was observed during the first hours of Con A-induced hepatitis (Figure 2E). The IL-6 serum levels returned to basal levels 24 hours after Con A injection. IL-6 pretreatment reduced IL-6 serum levels at later time points (Figure 2E). A different IL-6 kinetic was evident in alfpCre gp130^{LoxP/LoxP} animals. In both groups, a marked increase in IL-6 serum levels was obvious during the first hours after Con A injection. Additionally, IL-6 remained elevated during the first 24 hours in both groups (Figure 2F).

The IL-6–gp130-dependent activation of STAT3 in wild-type mice is suppressed in alfpCre gp130^{LoxP/LoxP} animals. To distinguish between the intracellular events that occur in wild-type and alfpCre gp130^{LoxP/LoxP} animals during Con A-induced liver cell damage, we analyzed hepatic STAT1 and STAT3 activation during disease progression. Earlier studies indicated that STAT1 plays a harmful role during activation of CD4⁺ and NKT cells (29). Therefore, we studied nuclear translocation of phosphorylated STAT1 and STAT3 in the liver.

IL-6 pretreatment had no impact on hepatic STAT1 activation in wild-type or in alfpCre gp130^{LoxP/LoxP} mice (Figure 3A; 0 hours, Con A) (25). Con A injection resulted in STAT1 activation in wild-type and alfpCre gp130^{LoxP/LoxP} mice, but no remarkable differences were found between the 2 groups (Figure 3A). IL-6 pretreatment resulted in a slight increase of STAT1 phosphorylation in wild-type mice 2 hours and 4 hours after Con A injection (Figure 3A). In alfpCre gp130^{LoxP/LoxP} animals, IL-6 injection resulted in a stronger and earlier STAT1 phosphorylation than in wild-type mice. Eight hours after Con A injection, STAT1 activation returned to basal levels (Figure 3A).

Activation of STAT3 during Con A-induced hepatitis can be divided into 3 phases (Figure 3B). The prephase, before Con A injection (0 hours), the immediate phase, 2 hours after injection, and 2 later phases, 4 and 8 hours after initiation of the disease.

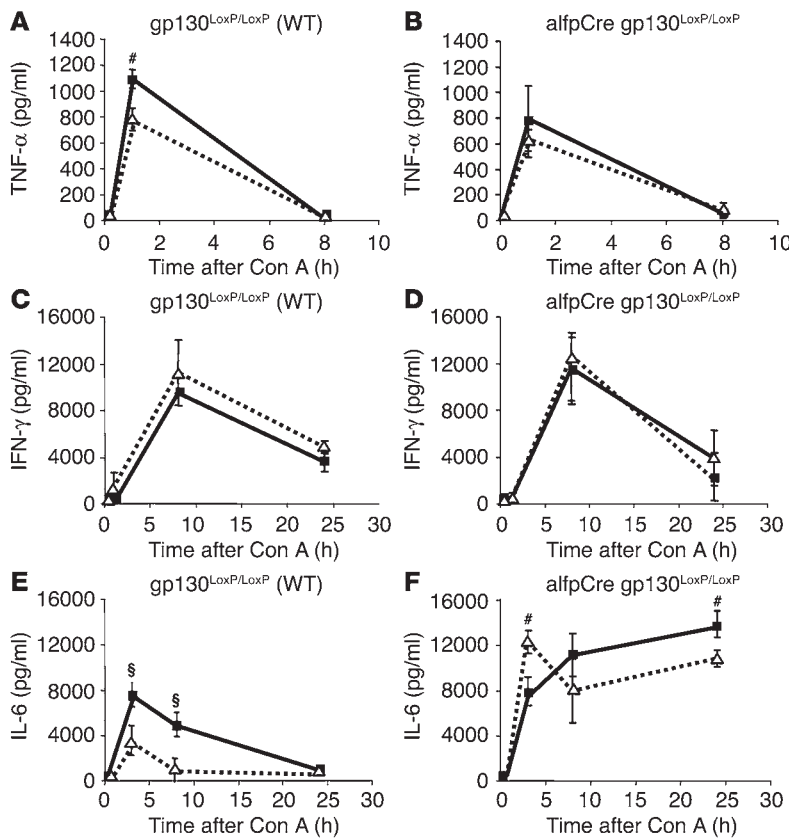


Figure 2 Cytokine secretion during Con A-induced hepatitis. Cytokine levels in the serum after Con A injection in wild-type (gp130^{LoxP/LoxP}) and alfpCre gp130^{LoxP/LoxP} mice. Three hours before Con A administration, animals were treated with NaCl (solid line) or IL-6 (200 μg/kg) (dotted line) by i.p. injection. (A and B) TNF-α levels of wild-type and alfpCre gp130^{LoxP/LoxP} mice. #P < 0.01 vs. corresponding IL-6-pretreated wild-type control group at the same time point. (C and D) IFN-γ levels of wild-type and alfpCre gp130^{LoxP/LoxP} mice. (E and F) IL-6 concentrations of wild-type and alfpCre gp130^{LoxP/LoxP} mice. §P < 0.001 and #P < 0.01 vs. corresponding IL-6-pretreated wild-type or alfpCre gp130^{LoxP/LoxP} mice at the same time point.

To differentiate between STAT3 activation in hepatocytes and other liver cells we performed coimmunofluorescence stainings of CD11b and P-STAT3. In the prephase, STAT3α phosphorylation was exclusively detectable in hepatocytes of IL-6-pretreated wild-type animals, but not in IL-6-injected alfpCre gp130^{LoxP/LoxP} animals (Figure 3B; 0 hours, Con A).

Two hours after Con A injection, IL-6 pretreatment resulted in stronger STAT3α activation in wild-type and alfpCre gp130^{LoxP/LoxP} animals compared to that in the NaCl-treated groups (Figure 3B). During this phase, STAT3 was predominately expressed in activated monocytes, NK cells, and macrophages (Figure 3C; CD11b⁺ cells). IL-6 pretreatment enhanced the number of STAT3-positive cells (Figure 3C).

At the later phase, 4 hours after Con A injection, strong P-STAT3α and P-STAT3β signals were found exclusively in hepatocytes of NaCl-treated wild-type mice. This strong STAT3 activation was found in neither of the other groups (Figure 3, B and D). Increased STAT3 activation 4 hours after Con A injection depended on gp130 expression in hepatocytes. IL-6 pretreatment reduced STAT3 activation in hepatocytes in wild-type animals (Figure 3D). In hepatocyte-

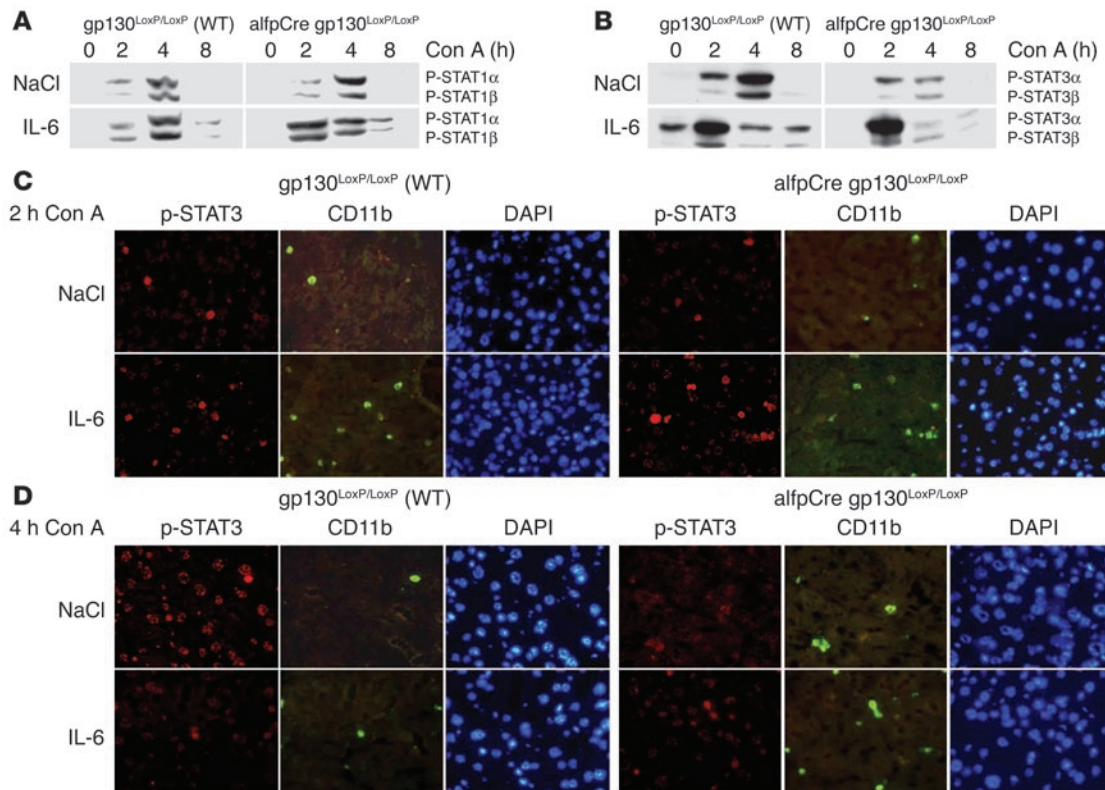
specific gp130^{-/-} mice, only a weak STAT3 activation in nonparenchymal liver cells (CD11b⁺ cells) was detectable. This activation was independent of IL-6 pretreatment (Figure 3D).

Generation and molecular characterization of hepatocyte-specific gp130^{ASTAT/LoxP} and gp130^{Y757F/LoxP} mice. Since gp130 expression in hepatocytes is essential for IL-6-induced protection in Con A-induced hepatitis, we aimed to identify the intracellular signaling pathways that are responsible for mediating protection. For this purpose, we generated mice with hepatocyte-specific deletions of either gp130-STAT1/3 or gp130-SHP2-RAS-MAPK signaling. The activation of the 2 distinct signaling cascades in response to ligand-mediated gp130 dimerization is mediated by phosphorylation of specific tyrosines (Y) in the cytoplasmic domain of gp130. Y757 mediates the engagement of the cytoplasmic Src-homology tyrosine phosphatase (SHP2) and the activation of the RAS-ERK pathway (30). The 4-membrane distal phosphotyrosines are binding sites for the SH2 domains of the latent transcription factors STAT1 and STAT3 (31).

The alfpCre gp130^{ASTAT/LoxP} and alfpCre gp130^{Y757F/LoxP} animals were obtained by crossing alfpCre gp130^{LoxP/LoxP} with either gp130^{ASTAT/ASTAT} or gp130^{Y757F/Y757F} knockin mice (32). Gp130^{ASTAT/ASTAT} mice express a truncated gp130 protein that lacks the part of the cytoplasmic domain required for STAT1 and STAT3 binding and activation. Gp130^{Y757F/Y757F} animals express a gp130 protein with a phenylalanine substitution of the Y757 residue which, in its phosphorylated form, is essential for SHP2 recruitment and subsequent activation of the RAS-MAPK cascade. In the resulting alfpCre gp130^{ASTAT/LoxP} and alfpCre gp130^{Y757F/LoxP} animals, the LoxP-flanked gp130 is deleted selectively in hepatocytes as expression of Cre recombinase is controlled by a hepatocyte-specific promoter (25). This approach therefore enables the selective expression of mutant gp130 protein in hepatocytes. Each mouse was genotyped by PCR analysis for the genomic existence of Cre, gp130^{LoxP}, and the respective mutant gp130 allele.

Functional characterization of the alfpCre gp130^{ASTAT/LoxP} and alfpCre gp130^{Y757F/LoxP} animals was performed by IL-6 stimulation in primary hepatocytes isolated from the 4 strains. IL-6-induced activation of gp130-dependent pathways was studied by the monitoring of P-STAT1/3 and P-ERK2 expression. Treatment of wild-type primary hepatocytes resulted in phosphorylation of STAT3 and ERK2 (Figure 4B). Neither protein was phosphorylated (and hence activated) in hepatocytes derived from alfpCre gp130^{LoxP/LoxP} mice (Figure 4C). However, in hepatocytes isolated from IL-6-stimulated alfpCre gp130^{Y757F/LoxP} or alfpCre gp130^{ASTAT/LoxP} mice, we observed selective activation of P-STAT3 or P-ERK2, respectively (Figure 4, D and E). P-STAT1 activation was neither induced in IL-6-stimulated primary hepatocytes isolated from wild-type, alfpCre gp130^{LoxP/LoxP}, alfpCre gp130^{Y757F/LoxP}, nor alfpCre gp130^{ASTAT/LoxP} animals (data not shown).

Activation of the IL-6-gp130-STAT pathway in hepatocytes confers protection during Con A-induced liver damage. We used alfpCre gp130^{Y757F/LoxP} and alfpCre gp130^{ASTAT/LoxP} animals to identify the

**Figure 3**

Changes in liver nuclear phosphorylation of STAT1 and STAT3 during Con A–induced hepatitis. **(A)** Phosphorylation of STAT1 in wild-type and alfpCre gp130^{LoxP/LoxP} mice. Western blot analysis of STAT1 and STAT3 activation, as detected by phosphorylation of STAT1 and STAT3, in liver nuclear protein extracts of wild-type and alfpCre gp130^{LoxP/LoxP} mice. Animals were pretreated 3 hours before Con A administration with NaCl or IL-6 (200 µg/kg) by i.p. injection as indicated. Representative results of 3 independent experiments are shown. **(B)** Phosphorylation of STAT3 in wild-type and alfpCre gp130^{LoxP/LoxP} mice. **(C)** Double immunofluorescence of liver sections for P-STAT3 and CD11b expression. CD11b detects activated macrophages, NK cells, and monocytes. Mice were killed 2 hours after Con A injection. DAPI counterstaining was used to detect nuclei. **(D)** Double immunofluorescence of liver sections for P-STAT3 and CD11b expression. CD11b detects activated macrophages, NK cells, and monocytes. Mice were killed 4 hours after Con A injection. Representative areas are shown. Slides of 3 animals per group were analyzed. Magnification, ×400.

gp130-dependent pathways in hepatocytes essential for mediating IL-6–dependent protection during Con A–induced hepatitis. IL-6 pretreatment of alfpCre gp130^{Y757F/LoxP} mice resulted in complete prevention of liver cell damage (Figure 5A). In contrast, alfpCre gp130^{ASTAT/LoxP} animals showed enhanced sensitivity toward Con A when compared to wild-type mice (Figure 5B). Independently of IL-6 pretreatment, all alfpCre gp130^{ASTAT/LoxP} mice died within 8 hours after Con A injection in contrast to a 100% survival rate for all analyzed alfpCre gp130^{Y757F/LoxP} animals.

To analyze possible modifications of immune-cell activation in these animals, serum TNF-α, IFN-γ, and IL-6 levels were determined before and after Con A injection (Figure 5, C and D). IL-6 pretreatment in alfpCre gp130^{Y757F/LoxP} or alfpCre gp130^{ASTAT/LoxP} animals had no significant impact on TNF-α serum levels (Figure 5D). In both mouse strains, IL-6 treatment resulted in slightly elevated IFN-γ serum levels (Figure 5, B and C). Additionally, IL-6 serum levels did not differ between the vehicle-treated alfpCre gp130^{Y757F/LoxP} and alfpCre gp130^{ASTAT/LoxP} animals. In both mouse strains, we detected maximal IL-6 concentrations 8 hours after Con A injection (Figure 5D). In contrast, pretreatment with recombinant IL-6 resulted in a reduction of endogenous IL-6 serum concentrations during Con A–induced hepatitis in alfpCre

gp130^{Y757F/LoxP} animals (Figure 5C). No reduction of IL-6 serum levels was observed in alfpCre gp130^{ASTAT/LoxP} mice (Figure 5D).

Gene expression profiles of IL-6–gp130 pathways in hepatocytes. The analysis of hepatocyte-specific gp130 mutations during Con A–induced hepatitis demonstrated that IL-6–gp130–STAT3–dependent signals appear to confer protection. To identify potential target genes involved in mediating protection, hepatic gene expression profiles were determined in IL-6–treated wild-type, alfpCre gp130^{LoxP/LoxP}, alfpCre gp130^{Y757F/LoxP}, and alfpCre gp130^{ASTAT/LoxP} mice. Figure 6 depicts a selection of genes that are significantly regulated by gp130-dependent pathways in hepatocytes *in vivo*. These can be divided into 2 groups: genes involved in controlling gp130-dependent signaling in the cell, e.g., *stat-1*, *stat-3*, *socs-1* (suppressor of cytokine signaling-1) and *socs-3*; and genes regulating immune-mediated mechanisms, e.g., serum amyloid A2 (*saa2*) and keratinocyte growth factor (*kc*). As the gp130-STAT3-dependent pathway confers protection in the Con A model, we hypothesized that indirect immune-mediated mechanisms were essential for protection against liver damage in the Con A model.

Treatment with SAA2 and KC protects against Con A–induced liver damage. We analyzed in more detail the regulation of *saa* and *kc* and their potential roles during Con A–induced liver failure. Both

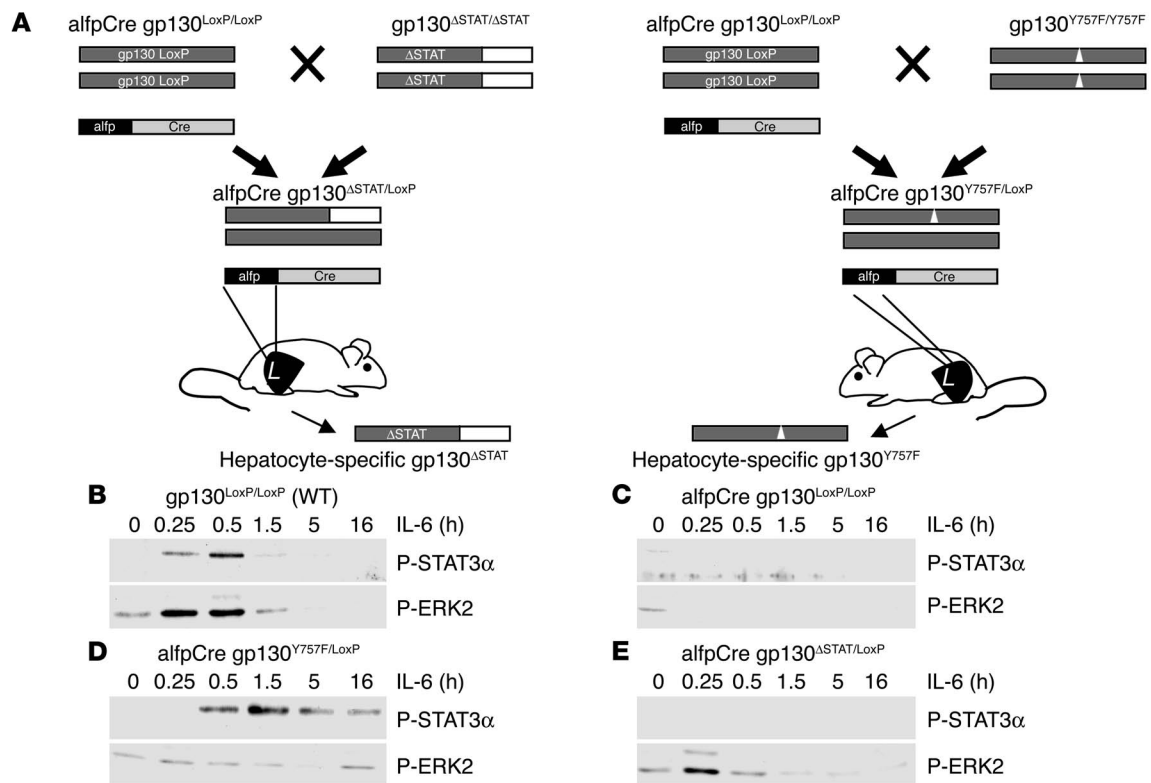


Figure 4

Generation and functional characterization of hepatocyte-specific gp130^{ΔSTAT/LoxP} and gp130^{Y757F/LoxP} mice. (A) alfpCre gp130^{LoxP/LoxP} mice were generated by breeding alfpCre mice with animals expressing LoxP-flanked gp130 alleles (25). Hepatocyte-specific gp130^{ΔSTAT/LoxP} animals (alfpCre gp130^{ΔSTAT/LoxP}) were generated by crossing alfpCre gp130^{LoxP/LoxP} with gp130^{ΔSTAT/ΔSTAT} mice, which express a truncated gp130 knockin allele encoding a truncated gp130 protein that lacks the domains mediating STAT1 and STAT3 activation (26). Hepatocyte-specific gp130^{Y757F/LoxP} animals (alfpCre gp130^{Y757F/LoxP}) were bred by crossing alfpCre gp130^{LoxP/LoxP} with gp130^{Y757F/Y757F} mice, which express a gp130 allele encoding a phenylalanine substitution of the Y757 residue (32), thereby rendering gp130 incapable of recruiting SHP2 and activating the RAS-MAPK pathway. Animals were genotyped by PCR analysis for alfpCre, gp130^{LoxP}, and gp130^{Y757F} alleles. (B and E) The functional characterization of hepatocyte-specific gp130 mutant mice. Gp130 downstream-signaling pathways were analyzed by monitoring of phosphorylated STAT3 and phosphorylated ERK2 (p42) expression in whole cell extracts of primary hepatocytes isolated from wild-type (B), alfpCre gp130^{LoxP/LoxP} (C), alfpCre gp130^{Y757F/LoxP} (D), or alfpCre gp130^{ΔSTAT/LoxP} mice (E). Activation of phosphorylated STAT1 was not detected in any of the 4 mouse strains.

genes are selectively induced via IL-6–gp130–STAT3. The analysis of SAA serum expression showed that pronounced transcriptional induction of the *saa* gene strictly depended on IL-6–gp130–STAT3 signaling in hepatocytes. In order to confirm the array analysis, we also investigated hepatic mRNA expression (data not shown) and serum levels of SAA and found that both were elevated only in wild-type and alfpCre gp130^{Y757F/LoxP} mice (Figure 7A).

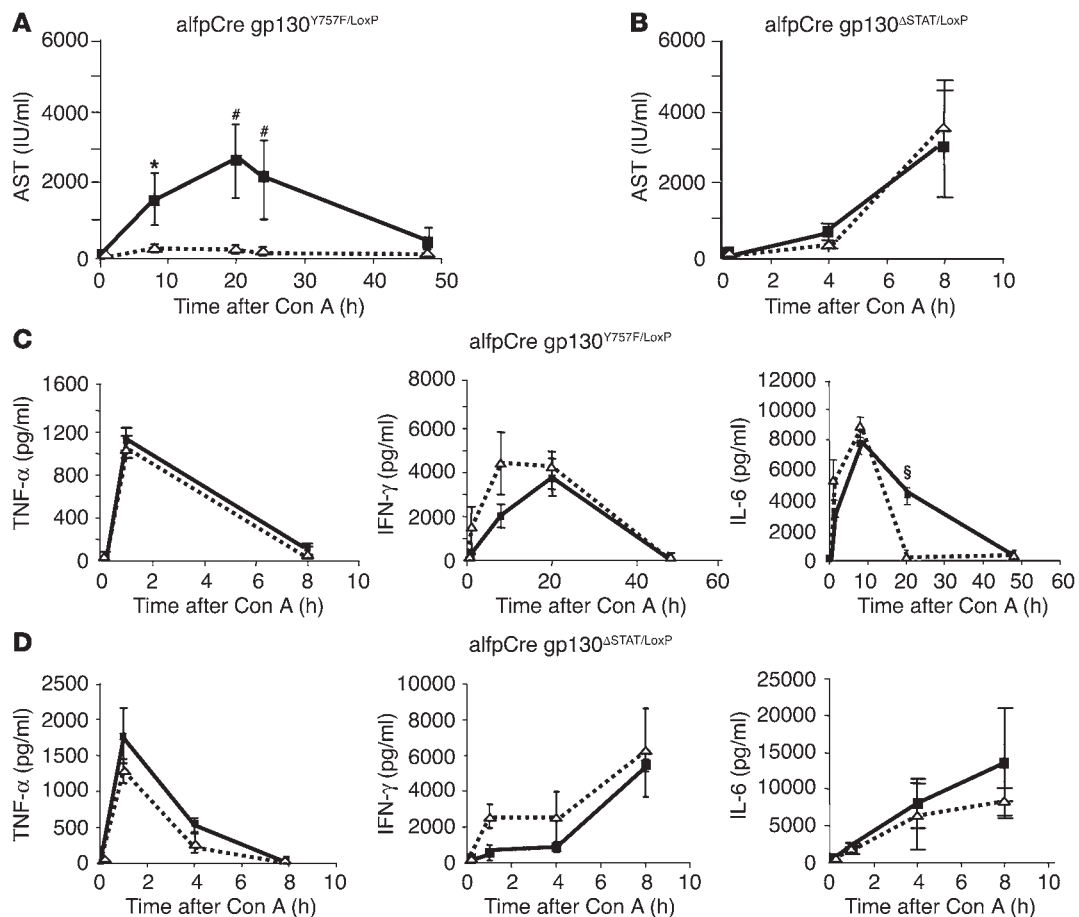
SAA is known to interact with metalloproteinases and to influence the activity of immune cells (33). Therefore, we studied the impact of SAA on Con A–induced hepatitis by pretreating wild-type animals with recombinant SAA 1 hour before Con A injection. SAA injection resulted in a significant reduction in the increase of AST levels compared with those in vehicle-treated control animals, indicating that SAA may have a protective effect for Con A–induced liver damage (Figure 7B).

KC controls chemotaxis and activation of polymorph nuclear cells (PMNs) in areas of inflammation. Serum KC expression was also strictly dependent on an intact IL-6–gp130–STAT3–signaling axis in hepatocytes (Figures 6 and 7C). No hepatic KC regulation was found in alfpCre gp130^{ΔSTAT3/LoxP} and alfpCre gp130^{LoxP/LoxP} animals. Earlier results showed that the preexistence of high KC

concentration in the serum leads to decreased PMN infiltration during inflammation (34). This effect is caused by reduced sensitivity of downstream pathways of the corresponding chemokine receptor (34). We thus analyzed the influence of IL-6 pretreatment on PMN infiltration during Con A–induced hepatitis. IL-6 treatment resulted in a significant reduction of PMN infiltration 4 hours after Con A injection (Figure 7D). This time coincided with the maximum of PMN infiltration. In order to further investigate the relevance of this observation, recombinant KC was injected before Con A administration. KC had a protective effect on Con A–induced T cell–mediated liver failure. The increase in transaminases was significantly blocked in the animals treated with KC (Figure 7E). Additionally, KC treatment leads to 100% survival during Con A–induced hepatitis compared with 70% in NaCl-treated animals.

Discussion

Con A injection into mice results in T cell activation in the liver as well as hepatocyte damage. The mechanisms during Con A–induced disease progression resemble human liver diseases, e.g., autoimmune disease and viral hepatitis (12–18). Therefore, the

**Figure 5**

gp130-STAT3 signaling in hepatocytes is responsible for IL-6–induced liver protection. Con A–induced hepatitis was induced by intravenous injection of 32.5 mg/kg Con A in hepatocyte-specific gp130^{ΔSTAT} (*alfpCre gp130^{ΔSTAT/LoxP}*) and hepatocyte-specific gp130^{Y757F} (*alfpCre gp130^{Y757F/LoxP}*) mice (*alfpCre gp130^{Y757F/LoxP}*). Mice were pretreated 3 hours before Con A injection with NaCl (solid line) or IL-6 (200 ng/g) by i.p. injection. (A and B) Liver damage was quantified by detection of ASTs. (A) AST levels of *alfpCre gp130^{Y757F/LoxP}* mice in the time course of Con A–induced hepatitis, pretreated with NaCl (solid line) or IL-6 (dotted line). **P* < 0.01 and **P* < 0.05 vs. corresponding IL-6–pretreated control group at the same time point. (B) AST levels of *alfpCre gp130^{ΔSTAT/LoxP}* in the time course of Con A–induced hepatitis, pretreated with NaCl (solid line) or IL-6 (dotted line). (C and D) TNF-α, IFN-γ, and IL-6 secretion in the serum during Con A–induced hepatitis in *alfpCre gp130^{Y757F/LoxP}* (C) and *alfpCre gp130^{ΔSTAT/LoxP}* mice (D) was determined by ELISA. §*P* < 0.001 vs. corresponding IL-6–pretreated *alfpCre gp130^{Y757F/LoxP}* mice at the same time point.

model is attractive for exploring mechanisms that might ultimately result in new therapeutic options.

We analyzed mice with mutations in the gp130 receptor in hepatocytes that selectively impair the signaling capacity of this receptor. Functional inactivation of this molecule in hepatocytes resulted in lack of signal activation after stimulation with ligands of the IL-6 cytokine family, e.g., IL-6 or OSM. Further experiments in hepatocyte-specific knockout animals showed that lack of gp130 expression in hepatocytes renders these animals more susceptible to injury during various pathophysiological conditions of the liver (25). Therefore, the aim of the present study was to identify molecular mechanisms that are involved in mediating IL-6–gp130–dependent protection in hepatocytes.

Earlier studies demonstrated that IL-6 attenuated liver injury in Con A–induced hepatitis (1). Additionally, recent reports demonstrated that other IL-6 family members, e.g., IL-11 and CT-1, also confer protection in this model (35, 36). As all IL-6 family members use the gp130 receptor for signal transduction, our aim was to deter-

mine the cell type that confers protection in this model. Interestingly, when gp130 was selectively deleted in hepatocytes, IL-6 no longer conferred a protective effect (Figure 1). Moreover, in hepatocyte-specific gp130 knockout mice, Con A–induced liver injury was more pronounced and resulted in death of the animals within 24 hours, indicating that gp130-dependent pathways in liver cells are also protective in the later phase of Con A–induced liver injury.

In a recent study, Sun et al. also suggested that IL-6 might attenuate liver injury in Con A–induced hepatitis (37) by suppressing the activity of NKT cells. NKT cell activation is an important event in the initial phase of Con A–induced hepatitis (38). However, the IL-6 doses Sun et al. used were 10-fold higher than in the IL-6–treatment schedule used in this study. Thus, the effect of IL-6 on NKT cell activation might be added to the more prominent effect triggered by IL-6 in hepatocytes.

Intracellular signaling mediated by gp130 is dependent on phosphorylation of tyrosine residues in the intracellular part of the receptor. To dissect the contribution of the 2 major pathways engaged by



Gene ID	gp130 ^{LoxP/LoxP} (WT)	alfpCre gp130 ^{LoxP/LoxP}	alfpCre gp130 ^{Y757F/LoxP}	alfpCre gp130 ^{ΔSTAT/LoxP}
SAA2	++++	+	++++	–
KC (Gro1-α)	+++		++	--
SOCS-3	+++	++	+++	
STAT3	++		+	
STAT1	+		+	
LBP	++		++	
Fibronectin	++	--	++	–
IL-6 α				++
p450	–	+	–	----
Glycine R				++++

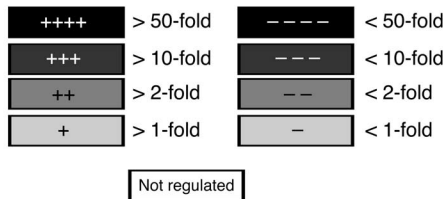


Figure 6

IL-6-induced gene expression profile of wild-type, alfpCre gp130^{LoxP/LoxP}, alfpCre gp130^{Y757F/LoxP}, and alfpCre gp130^{ΔSTAT/LoxP} mice. Affimetrix GeneChip analysis was used to detect gene expression of IL-6-stimulated gp130^{LoxP/LoxP}, alfpCre gp130^{LoxP/LoxP}, alfpCre gp130^{ΔSTAT/LoxP}, and alfpCre gp130^{Y757F/LoxP} mice. Three animals per group were treated in parallel by i.p. injection of recombinant IL-6 (IL-6 α) (200 μ g/kg) or NaCl. Liver RNA was isolated, and gene expression was compared. Most of the examples shown are differentially regulated by gp130-STAT signaling. Glycine receptor (Glycine R) and cytochrome p450 (p450) represent examples that are regulated by gp130-ras-MAPK signaling. The change of gene expression level is marked by increasing color intensity. LBP, LPS binding protein.

gp130 activation, we combined gp130 knockin mutant animals with tissue-specific gp130 knockout animals in order to genetically restrict the capacity of gp130 to selectively activate only 1 of these 2 pathways in hepatocytes *in vivo*. Since this strategy relies on monoallelic expression of gp130, it is important to ensure that this manipulation does not confer the rate-limiting step for IL-6 signaling in hepatocytes. We have previously shown that the rate-limiting step during IL-6-dependent signal transduction in this cell type is in fact expression of gp80 on the cell surface (39, 40), and monoallelic ablation of gp130 by the LoxP/Cre technology did not change the strength of STAT3 activation after IL-6 stimulation (25). Experiments in primary hepatocytes isolated from these animal strains demonstrated that our concept is valid. Therefore, we addressed the question of which of the 2 gp130-mediated intracellular pathways is essential to trigger IL-6-dependent liver protection during Con A-induced hepatitis.

IL-6 stimulation of alfpCre gp130^{ΔSTAT/LoxP} and alfpCre gp130^{Y757F/LoxP} animals revealed that phosphorylation of the 4 membrane distal tyrosine residues in gp130 that mediate activation of STAT3 are required to attenuate Con A-induced liver injury while the gp130-SHP2-RAS-MAPK pathway appears to be completely dispensable in mediating this effect. Interestingly, in our present and former experiments, IL-6 and OSM stimulation did not trigger STAT1 activation in the liver (25). Therefore, our findings indicate that the protective effects are mediated by STAT3.

In further experiments, we analyzed whether IL-6 pretreatment induces changes in gp130-dependent signaling in hepatocytes. IL-6 stimulation may have effects on cytokine secretion during Con A-induced hepatitis. In particular, TNF- α and IFN- γ have been shown to play an essential role (41, 42). TNF- α is produced primarily by Kupffer cells in Con A-induced hepatitis (16). In wild-type mice, TNF- α levels were reduced after IL-6 stimulation. But in alfpCre gp130^{Y757F/LoxP} mice, which retained sensitivity to IL-6-dependent liver protection, no changes in TNF- α levels were detected. These results indicate that a change in TNF- α serum levels is not essential for the protective effect mediated by IL-6.

IFN- γ is a marker of activated CD4⁺ cells and is strongly elevated after Con A injection (27, 42). IFN- γ levels in alfpCre gp130^{Y757F/LoxP} and wild-type mice were not affected by pretreatment with IL-6, despite our observation that both strains showed protection from Con A-induced liver damage (Figure 2, C and D; Figure 5, C and D). Thus, serum levels of TNF- α and IFN- γ showed no correlation with the capacity of IL-6 to provide protection from liver damage, indicating that alterations in concentrations of these cytokines are unlikely to explain protection.

We next concentrated on mechanisms related to IL-6-dependent signaling in hepatocytes. IL-6 serum concentrations correlated with survival rates. High IL-6 serum concentrations after Con A injection were detectable in animals with a disruption of the IL-6-gp130-STAT3 pathway and correlated with increased morbidity. In contrast, IL-6-induced activation of STAT3 in hepatocytes prior to or 4 hours after Con A challenge was associated with survival of the animals. Lack of STAT3 activation in hepatocytes at these time points, as observed in alfpCre gp130^{LoxP/LoxP} (Figure 1B) and alfpCre gp130^{ΔSTAT/LoxP} (Figure 5B) animals, correlated with poor prognosis.

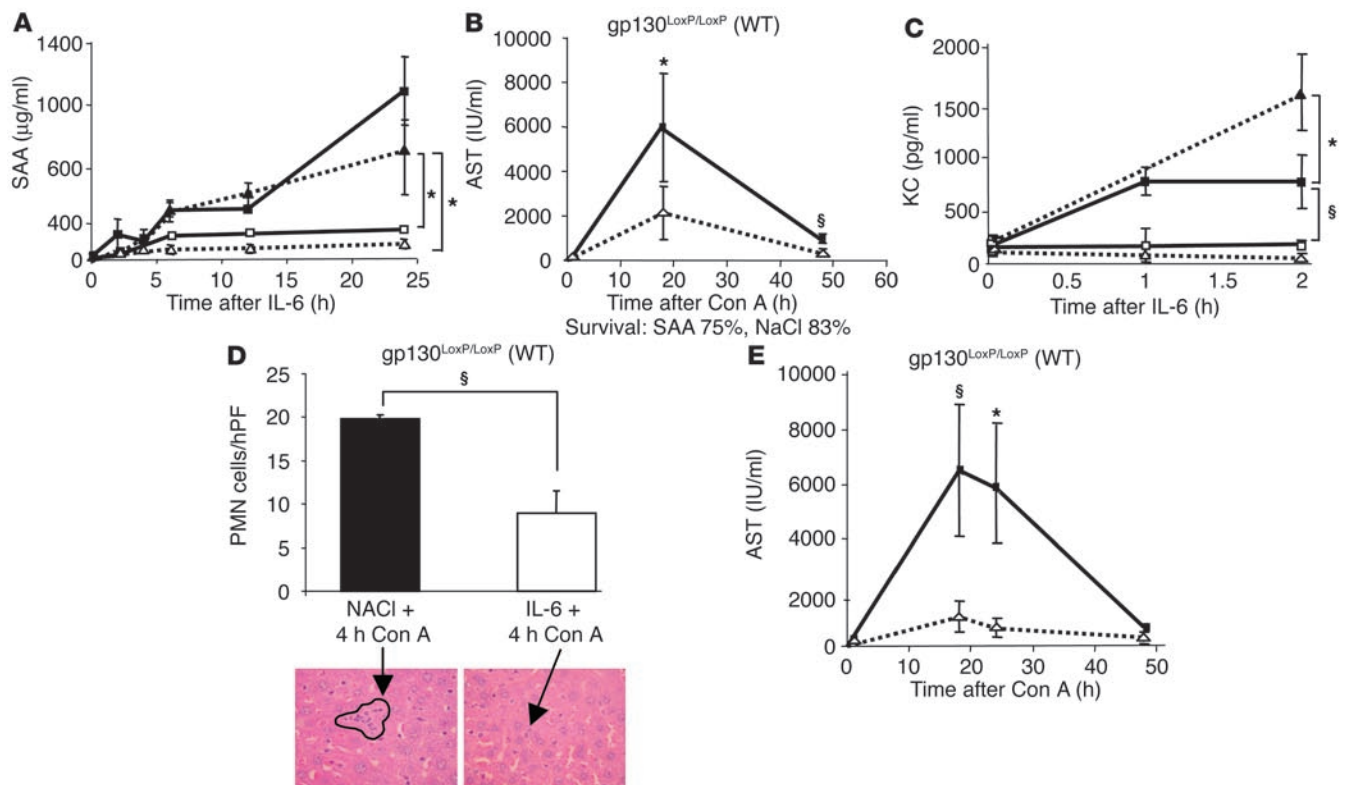
STAT3 activation 2 hours after Con A injection occurred predominantly in activated immune cells, such as NK cells and infiltrating monocytes (CD11b⁺ cells) (Figure 3C, NaCl-treated groups). The pathways leading to STAT3 activation in these cells are currently unclear. gp130-dependent or gp130-independent factors, e.g., IFN- γ , could be relevant in explaining this observation (29).

IL-6 pretreatment increased the amount of phosphorylated STAT3 in nonparenchymal cells 2 hours after Con A injection by increasing numbers of P-STAT3-positive cells (Figure 3C). The increased number of STAT3-positive cells likely reflects IL-6-induced sensitization of NK cells, monocytes, or Kupffer cells to STAT3-activating pathways.

Four hours after Con A injection, STAT3 activation occurred predominantly in hepatocytes in a gp130-dependent manner (Figure 3, B and D). Strong STAT3 activation in this phase correlated with maximal IL-6 serum levels (Figure 2E). IL-6 pretreatment inhibited the increase of STAT3 activation in hepatocytes of wild-type mice, probably by inducing negative feedback mechanisms, e.g., induction of SOCS-3 in hepatocytes (Figure 6).

It has been shown that SOCS-3 negatively regulates IL-6 signaling *in vivo* (43). In agreement with these findings, we demonstrated that activation of STAT3 is transitional. Hepatocytes of IL-6-pretreated wild-type mice showed STAT3 activation 3 hours after IL-6 injection. Up to 4 hours after initiation of Con A-induced hepatitis, these cells were not able to activate STAT3, although high IL-6 serum levels were detectable (Figures 3D and 2E).

In order to define potential IL-6-gp130-STAT3 target genes in hepatocytes that might be involved in conferring protection during Con A-induced liver failure, we performed gene expression profiling. Interestingly some acute phase genes were strictly

**Figure 7**

Acute-phase protein SAA2 and the chemokine KC are IL-6-gp130-STAT-induced, liver-protective proteins. (A) SAA2 serum levels after IL-6 (200 µg/kg) injection. Each time point represents the serum of 3–5 animals. Filled squares represent wild-type mice, open squares show alp1Cre gp130^{LoxP/LoxP} mice, filled triangles mark alp1Cre gp130^{Y757F/LoxP} mice, and open triangles represent alp1Cre gp130^{ASTAT/LoxP}. (B) Pretreatment with recombinant SAA (0.8 mg/kg) leads to a significant reduction of AST levels in the time course of Con A-induced hepatitis in wild-type mice. Either SAA (dotted line) or NaCl (solid line) was injected intravenously 1 hour before induction of Con A-induced hepatitis. (C) Serum KC levels after IL-6 injection. Filled squares represent wild-type mice, open squares show alp1Cre gp130^{LoxP/LoxP} mice, filled triangles mark alp1Cre gp130^{Y757F/LoxP} mice, and open triangles represent alp1Cre gp130^{ASTAT/LoxP}. (D) IL-6 treatment results in a significant reduction of PMN infiltration during Con A-induced hepatitis. Four hours after Con A injection, the influx of PMNs was counted on H&E-stained paraffin sections by an experienced liver pathologist. The arrows mark liver infiltrating PMNs. hPF, high powered field. (E) KC (40 µg/kg) treatment leads to a significant reduction of AST levels during Con A-induced hepatitis. Eight mice per group were treated with either KC (dotted line) or NaCl (solid line) 1 hour before Con A injection. §*P* < 0.001 and **P* < 0.05 vs. corresponding control groups at the same time point.

regulated via IL-6-gp130-STAT3. SAA2 showed the most prominent regulation. SAA2 is a known target of MMP and MMP activity induced during T cell-mediated hepatitis. Earlier experiments have shown that inhibition of MMPs attenuates liver failure (44). Indeed, treatment with recombinant SAA2 attenuated Con A-induced liver injury (Figure 7B). Therefore, one of the mechanisms through which SAA2 might be protective is substrate competition of MMP activity.

Activation of PMNs during Con A-induced liver failure is an essential step for disease progression (12). IL-6-treated mice showed a significant reduction in PMN infiltration during Con A-induced hepatitis (Figure 7D). Results of the gene expression analysis are remarkable in this context, as the CXC chemokine KC was strongly upregulated in response to activation of the IL-6-gp130-STAT3 pathway. KC is an immediate early gene with low or no detectable expression in most tissues. A variety of factors, such as LPS or PDGF, induce tissue-specific expression of KC (45), which in turn promotes localized PMN migration. However, KC alone is not sufficient for the activation of infiltrated cells, and high systemic KC levels lead to impaired PMN activa-

tion via desensitization of the PMN CXC-receptor 2 (46). IL-6 stimulation induces KC serum levels by approximately 100-fold, correlating with a pronounced upregulating of KC mRNA in the liver (Figure 6). But IL-6-dependent hepatic KC expression by itself induces no influx of PMNs in the liver (data not shown). Our present analysis shows that KC confers protection in Con A-induced T cell-mediated hepatitis. These results indicate that high systemic KC levels directly attenuate immune cell activation, most likely via modulating PMN function. Additionally, recent studies showed effects of KC expression on monocyte recruitment during development of experimental atherosclerosis (47). Also, modulation of liver monocyte activation might be a mechanism by which the chemokine prevents Con A-induced liver damage. KC-mediated mechanisms might be of general interest for the study of various liver-damaging conditions and will be the subject of further research.

In conclusion, our present analysis suggests that IL-6-gp130-dependent gene activation in hepatocytes confers protection against T cell hepatitis induced by Con A. Functional dissection of gp130-dependent pathways in hepatocytes demonstrates that



IL-6-mediated STAT3 activation correlates with reduced liver damage and induces hepatic expression of liver-protective proteins SAA2 and KC. Both proteins are potent inhibitors of Con A-induced hepatitis and might also be of interest in the treatment of immune-mediated liver diseases in humans.

Methods

Animals

Specified pathogen-free 8- to 10-week-old male BALB/c mice were obtained from the Animal Research Institute of the Medizinische Hochschule Hannover. H. Hedrich, state head of the animal facility at the Hannover Medical School, approved the care of animals and experiments. For each time point and group, 3–5 animals were treated in parallel.

Generation and genotyping of gp130-mutated animals

AlfpCre gp130^{LoxP/LoxP}. Hepatocyte-specific gp130^{-/-} mice were generated by breeding *alfpCre* mice with mice expressing LoxP-flanked gp130 alleles. Genomic DNA was isolated and analyzed by PCR as described previously (25). Gp130^{LoxP/LoxP} mice without Cre expression were used as control (wild-type) animals.

AlfpCre gp130^{ASTAT/LoxP}. Hepatocyte-specific gp130^{ASTAT/LoxP} animals were generated by breeding *alfpCre gp130^{LoxP/LoxP}* with gp130^{ASTAT/ASTAT} knockin mice. Gp130^{ASTAT/ASTAT} expresses a truncated gp130 knockin allele that lacks the essential region for the activation of STAT1 and -3 signaling (48). The genotype was detected by PCR analysis for *alfpCre*, gp130^{LoxP}, and gp130^{ASTAT} allele as described previously (32, 48).

AlfpCre gp130^{Y757F/LoxP}. Hepatocyte-specific gp130^{Y757F/LoxP} animals were generated by crossing *alfpCre gp130^{LoxP/LoxP}* with gp130^{Y757F/Y757F} knockin mice. The gp130^{Y757F/Y757F} mice express a gp130 allele with a point mutation at Y757. The Y757 is the essential tyrosine for the recruiting of SHP2 and the activation of downstream signals of the RAS-MAPK cascade (32). The genotype was analyzed by PCR analysis for *alfpCre*, gp130^{LoxP}, and gp130^{Y757F} allele as described previously (25, 32).

IL-6, SAA, KC, and Con A treatment

Con A-induced hepatitis was induced by intravenous injection of 32.5 mg/kg Con A. IL-6 (200 µg/kg) was injected i.p. 3 hours before Con A injection. Recombinant SAA (0.8 mg/kg) and recombinant KC (40 µg/kg) were applied by i.v. injection 1 hour before Con A administration. Control animals were injected with an equal volume of carrier solution (NaCl). Livers of IL-6-treated animals used for array analysis (at 0 hours) were perfused. To ensure that infiltrated cells in livers of Con A-treated mice were not eliminated, we washed the organs intensively by shaking the organs for 15 minutes in cold PBS.

Preparation of liver nuclear extracts

Liver nuclear extracts were prepared as described previously (49).

Quantification of hepatic PMNs

Sections of the livers of 4 mice per group were analyzed. From each liver slide, PMNs in 6 representative high-power fields were counted on an H&E stain by an experienced liver pathologist. Student's *t* test was performed to evaluate the significance of detected differences.

Detection of nuclear p-STAT3, p-STAT1, and p-ERK

Activated STAT and ERK were analyzed by detection of phosphorylated nuclear proteins. Five µg of liver nuclear proteins were separated on a 10% SDS-polyacrylamide gel and blotted onto nitrocellulose membrane. Phospho-STAT3 and phospho-STAT1 expression were analyzed by Western

blot, using an antibody directed against tyrosine phosphorylated STAT3 or STAT1 (Cell Signaling Technology). Phospho-ERK1/2 expression was analyzed by use of an antibody directed against phosphorylated ERK1/2 (Cell Signaling Technology). The antigen-antibody complexes were visualized using the ECL detection system as recommended by the manufacturer (Amersham Biosciences). To verify equal loading of protein samples, a Coomassie-blue stained SDS Gel was quantified.

Detection of p-STAT3 and CD11b⁺ cells

Cryosections of frozen livers were performed and slides were fixed in a combination of methanol and acetone. We performed CD11b-P-STAT3 double immunofluorescence staining. CD11b reacts to activated macrophages and Con A-activated monocytes. It thus serves as a marker for differentiation between STAT3-positive hepatocytes and STAT3-positive Con A-activated immune cells. CD11b-P-STAT3 double staining was performed by using rat anti-mouse CD11b antibody (BD Biosciences – Pharmingen) in combination with rabbit anti-mouse P-STAT3 (Cell Signaling Technology). As a second antibody, a mix of Alexa Fluor 488 donkey anti-rat and Alexa Fluor 594 donkey anti-rabbit was used (Molecular Probes).

Determination of IL-6, TNF-α, IFN-γ, KC, and SAA concentrations and AST activity

Blood was withdrawn by retro-orbital puncture at the indicated time points. TNF-α, IL-6, IFN-γ, KC, and SAA serum concentrations were detected by ELISA (mouse TNF; BD Biosciences – Pharmingen), mouse IL-6 (BD Biosciences – Pharmingen), mouse SAA (BioSource International), mouse KC (R&D Systems) as described previously (3).

Determination of ASTs

AST activity was determined by an automated enzyme assay as described previously (3).

Recombinant proteins

Recombinant IL-6 was produced and provided by S. Rose-John. Recombinant SAA was purchased from Cell Sciences. Recombinant KC was purchased from Strathmann Biotec AG.

Gene expression profile analysis

Affymetrix mouse genome GeneChip arrays were used to analyze gene expression of IL-6-stimulated gp130^{LoxP/LoxP} (wild-type), *alfpCre gp130^{LoxP/LoxP}*, *alfpCre gp130^{ASTAT/LoxP}*, and *alfpCre gp130^{Y757F/LoxP}* mice. Three animals per group were treated in parallel by i.p.-injected recombinant IL-6 (200 µg/kg) or NaCl. After 3 hours, animals were sacrificed. Liver RNA was isolated by guanidine isothiocyanate isolation. The RNA was used for the Affymetrix GeneChips, as described in the manufacturer's protocol. RNA of 3 mice per group was pooled. For each mouse strain, we compared mice treated with NaCl for 3 hours with those treated with IL-6 for 3 hours. Additionally, nuclear proteins were isolated from each liver, and the activation of STAT3 and ERK1/2 was analyzed by Western blot to verify the integrity of IL-6 signaling in each mouse.

Isolation and stimulation of primary hepatocytes

Primary mouse hepatocytes were isolated by collagenase perfusion (50). Mouse liver was perfused with HEPES buffer, then with collagenase solution, in a retrograde fashion. Isolated hepatocytes were washed with PBS. 1×10^6 cells were plated on 6 cm dishes in DMEM containing 10% fetal calf serum and a combination of penicillin and streptomycin. The medium was changed after 4 hours. The cells were cultured under serum-free conditions overnight. The next day, cells were stimulated with 200 ng/ml recombinant



IL-6. Cells were harvested at the indicated time points, and whole cell proteins, RNA, and nuclear proteins were isolated.

Acknowledgments

This work was supported by the Deutsche Forschungsgemeinschaft (SFB 566, Project B8).

Received for publication October 15, 2004, and accepted in revised form January 11, 2005.

Address correspondence to: Christian Trautwein or Christian Klein, Department of Gastroenterology, Hepatology and Endocrinology, Hannover Medical School, Carl-Neuberg-Strasse 1, 30625 Hannover, Germany. Phone: 49-511-532-6620; Fax: 49-511-532-5692; E-mail: Trautwein.Christian@mh-hannover.de (C. Trautwein). Phone: 49-511-532-3401; E-mail: klein.christian@mh-hannover.de (C. Klein).

Christian Klein and Torsten Wüstefeld contributed equally to this work.

- Mizuhara, H., et al. 1994. T cell activation-associated hepatic injury: mediation by tumor necrosis factors and protection by interleukin 6. *J. Exp. Med.* **179**:1529–1537.
- Kovalovich, K., et al. 2000. Increased toxin-induced liver injury and fibrosis in interleukin-6-deficient mice. *Hepatology*. **31**:149–159.
- Klein, C., et al. 2003. ME3738 protects from concanavalin A-induced liver failure via an IL-6-dependent mechanism. *Eur. J. Immunol.* **33**:2251–2261.
- Hong, F., et al. 2002. Elevated interleukin-6 during ethanol consumption acts as a potential endogenous protective cytokine against ethanol-induced apoptosis in the liver: involvement of induction of Bcl-2 and Bcl-x(L) proteins. *Oncogene*. **21**:32–43.
- Kovalovich, K., et al. 2001. Interleukin-6 protects against Fas-mediated death by establishing a critical level of anti-apoptotic hepatic proteins FLIP, Bcl-2, and Bcl-xL. *J. Biol. Chem.* **276**:26605–26613.
- Camargo, C.A., Jr., Madden, J.F., Gao, W., Selvan, R.S., and Clavien, P.A. 1997. Interleukin-6 protects liver against warm ischemia/reperfusion injury and promotes hepatocyte proliferation in the rodent. *Hepatology*. **26**:1513–1520.
- Sun, Z., et al. 2003. In vitro interleukin-6 treatment prevents mortality associated with fatty liver transplants in rats. *Gastroenterology*. **125**:202–215.
- Casini, A., Ricci, O.E., Paoletti, F., and Surrenti, C. 1985. Immune mechanisms for hepatic fibrogenesis. T-lymphocyte-mediated stimulation of fibroblast collagen production in chronic active hepatitis. *Liver*. **5**:134–141.
- Moebius, U., et al. 1990. T cell receptor gene rearrangements of T lymphocytes infiltrating the liver in chronic active hepatitis B and primary biliary cirrhosis (PBC): oligoclonality of PBC-derived T cell clones. *Eur. J. Immunol.* **20**:889–896.
- Ramadori, G., Moebius, U., Dienes, H.P., Meuer, S., and Meyer zum Buschenfelde, K.H. 1990. Lymphocytes from hepatic inflammatory infiltrate kill rat hepatocytes in primary culture. Comparison with peripheral blood lymphocytes. *Virchows Arch., B, Cell Pathol.* **59**:263–270.
- Trautwein, C., et al. 1998. Concanavalin A-induced liver cell damage: activation of intracellular pathways triggered by tumor necrosis factor in mice. *Gastroenterology*. **114**:1035–1045.
- Bonder, C.S., Ajuebor, M.N., Zbytniuk, L.D., Kubes, P., and Swain, M.G. 2004. Essential role for neutrophil recruitment to the liver in concanavalin A-induced hepatitis. *J. Immunol.* **172**:45–53.
- Dienes, H.P., Hutteroth, T., Hess, G., and Meuer, S.C. 1987. Immunoelectron microscopic observations on the inflammatory infiltrates and HLA antigens in hepatitis B and non-A, non-B. *Hepatology*. **7**:1317–1325.
- Russell, J.Q., et al. 1998. Liver damage preferentially results from CD8(+) T cells triggered by high affinity peptide antigens. *J. Exp. Med.* **188**:1147–1157.
- Sitia, G., et al. 2002. Depletion of neutrophils blocks the recruitment of antigen-nonspecific cells into the liver without affecting the antiviral activity of hepatitis B virus-specific cytotoxic T lymphocytes. *Proc. Natl. Acad. Sci. U. S. A.* **99**:13717–13722.
- Schumann, J., et al. 2000. Importance of Kupffer cells for T-cell-dependent liver injury in mice. *Am. J. Pathol.* **157**:1671–1683.
- Jaeschke, H. 2002. Neutrophil-mediated tissue injury in alcoholic hepatitis. *Alcohol*. **27**:23–27.
- Jaeschke, H., and Farhoo, A. 1991. Neutrophil and Kupffer cell-induced oxidant stress and ischemia-reperfusion injury in rat liver. *Am. J. Physiol.* **260**:G355–G362.
- Ishihara, K., and Hirano, T. 2002. Molecular basis of the cell specificity of cytokine action. *Biochim. Biophys. Acta*. **1592**:281–296.
- Stahl, N., et al. 1995. Choice of STATs and other substrates specified by modular tyrosine-based motifs in cytokine receptors. *Science*. **267**:1349–1353.
- Nakajima, K., et al. 1996. A central role for Stat3 in IL-6-induced regulation of growth and differentiation in M1 leukemia cells. *EMBO J.* **15**:3651–3658.
- Fukada, T., et al. 1996. Two signals are necessary for cell proliferation induced by a cytokine receptor gp130: involvement of STAT3 in anti-apoptosis. *Immunity*. **5**:449–460.
- Ernst, M., and Jenkins, B.J. 2004. Acquiring signaling specificity from the cytokine receptor gp130. *Trends Genet.* **20**:23–32.
- Rose-John, S. 2001. Coordination of interleukin-6 biology by membrane bound and soluble receptors. *Adv. Exp. Med. Biol.* **495**:145–151.
- Streetz, K.L., et al. 2003. Lack of gp130 expression in hepatocytes promotes liver injury. *Gastroenterology*. **125**:532–543.
- Betz, U.A., et al. 1998. Postnatally induced inactivation of gp130 in mice results in neurological, cardiac, hematopoietic, immunological, hepatic, and pulmonary defects. *J. Exp. Med.* **188**:1955–1965.
- Cao, Q., Batey, R., Pang, G., Russell, A., and Clancy, R. 1998. IL-6, IFN-gamma and TNF-alpha production by liver-associated T cells and acute liver injury in rats administered concanavalin A. *Immunol. Cell Biol.* **76**:542–549.
- Okamoto, T., et al. 1998. Expression of cytokine mRNA in extrahepatic organs in a mouse concanavalin A-hepatitis model. *Jpn. J. Pharmacol.* **77**:219–225.
- Hong, F., et al. 2002. Opposing roles of STAT1 and STAT3 in T cell-mediated hepatitis: regulation by SOCS. *J. Clin. Invest.* **110**:1503–1513. doi:10.1172/JCI200215841.
- Heinrich, P.C., Behrmann, I., Muller-Newen, G., Schaper, F., and Graeve, L. 1998. Interleukin-6-type cytokine signaling through the gp130/Jak/STAT pathway. *Biochem. J.* **334**:297–314.
- Taga, T., and Kishimoto, T. 1997. Gp130 and the interleukin-6 family of cytokines. *Annu. Rev. Immunol.* **15**:797–819.
- Tebbutt, N.C., et al. 2002. Reciprocal regulation of gastrointestinal homeostasis by SHP2 and STAT-mediated trefoil gene activation in gp130 mutant mice. *Nat. Med.* **8**:1089–1097.
- Stix, B., et al. 2001. Proteolysis of AA amyloid fibril proteins by matrix metalloproteinases-1, -2, and -3. *Am. J. Pathol.* **159**:561–570.
- Wiekowski, M.T., et al. 2001. Disruption of neutrophil migration in a conditional transgenic model: evidence for CXCR2 desensitization in vivo. *J. Immunol.* **167**:7102–7110.
- Bustos, M., et al. 2003. Protection against liver damage by cardiotrophin-1: a hepatocyte survival factor up-regulated in the regenerating liver in rats. *Gastroenterology*. **125**:192–201.
- Mahboubi, K., Biedermann, B.C., Carroll, J.M., and Pober, J.S. 2000. IL-11 activates human endothelial cells to resist immune-mediated injury. *J. Immunol.* **164**:3837–3846.
- Sun, R., Tian, Z., Kulkarni, S., and Gao, B. 2004. IL-6 prevents T cell-mediated hepatitis via inhibition of NKT cells in CD4+ T cell- and STAT3-dependent manners. *J. Immunol.* **172**:5648–5655.
- Toyabe, S., et al. 1997. Requirement of IL-4 and liver NK1+ T cells for concanavalin A-induced hepatic injury in mice. *J. Immunol.* **159**:1537–1542.
- Peters, M., Meyer zum Buschenfelde, K.H., and Rose-John, S. 1996. The function of the soluble IL-6 receptor in vivo. *Immunol. Lett.* **54**:177–184.
- Peters, M., et al. 1996. The function of the soluble interleukin 6 (IL-6) receptor in vivo: sensitization of human soluble IL-6 receptor transgenic mice towards IL-6 and prolongation of the plasma half-life of IL-6. *J. Exp. Med.* **183**:1399–1406.
- Gantner, F., Leist, M., Lohse, A.W., Germann, P.G., and Tiegs, G. 1995. Concanavalin A-induced T-cell-mediated hepatic injury in mice: the role of tumor necrosis factor. *Hepatology*. **21**:190–198.
- Nicoletti, F., et al. 2000. Essential pathogenetic role for interferon (IFN)-gamma in concanavalin A-induced T cell-dependent hepatitis: exacerbation by exogenous IFN-gamma and prevention by IFN-gamma receptor-immunoglobulin fusion protein. *Cytokine*. **12**:315–323.
- Crocker, B.A., et al. 2003. SOCS3 negatively regulates IL-6 signaling in vivo. *Nat. Immunol.* **4**:540–545.
- Wielockx, B., et al. 2001. Inhibition of matrix metalloproteinases blocks lethal hepatitis and apoptosis induced by tumor necrosis factor and allows safe antitumor therapy. *Nat. Med.* **7**:1202–1208.
- Bozic, C.R., et al. 1995. Expression and biologic characterization of the murine chemokine KC. *J. Immunol.* **154**:6048–6057.
- Lira, S.A., et al. 1994. Expression of the chemokine N51/KC in the thymus and epidermis of transgenic mice results in marked infiltration of a single class of inflammatory cells. *J. Exp. Med.* **180**:2039–2048.
- Huo, Y., et al. 2001. The chemokine KC, but not monocyte chemoattractant protein-1, triggers monocyte arrest on early atherosclerotic endothelium. *J. Clin. Invest.* **108**:1307–1314. doi:10.1172/JCI200112877.
- Ernst, M., et al. 2001. Defective gp130-mediated signal transducer and activator of transcription (STAT) signaling results in degenerative joint disease, gastrointestinal ulceration, and failure of uterine implantation. *J. Exp. Med.* **194**:189–203.
- Rakemann, T., et al. 1999. The designer cytokine hyper-interleukin-6 is a potent activator of STAT3-dependent gene transcription in vivo and in vitro. *J. Biol. Chem.* **274**:1257–1266.
- Gjessing, R., and Seglen, P.O. 1980. Adsorption, simple binding and complex binding of rat hepatocytes to various in vitro substrata. *Exp. Cell Res.* **129**:239–249.